

1 **Title:** Effects of Cone Penetrometer Testing on Shallow Hydrogeology at a Contaminated Site

2

3 **Authors:** Andrew D. Putt¹, Erin R. Kelly¹, Kenneth A. Lowe², Miguel Rodriguez Jr.² and Terry
4 C. Hazen^{1,2,3,4,5*}

5 ¹Department of Earth and Planetary Sciences, University of Tennessee, Knoxville, TN, USA

6 ²Biosciences Division, Oak Ridge National Laboratory, Oak Ridge, TN, USA

7 ³Department of Microbiology, University of Tennessee, Knoxville, TN, USA

8 ⁴Department of Civil and Environmental Sciences, University of Tennessee, Knoxville, TN,
9 USA

10 ⁵Institute for a Secure and Sustainable Environment, University of Tennessee, Knoxville, TN,
11 USA

12 *Corresponding author

13

14 **For Submission to ACS ES&T Engineering**

15

16 **The paper is a non-peer reviewed preprint submitted to EarthArXiv.**

17

18 **Abstract**

19 Penetration testing is a popular and instantaneous technique for subsurface mapping,
20 contaminant tracking, and the determination of soil characteristics. While the small footprint and
21 reproducibility of cone penetrometer testing makes it an ideal method for in-situ subsurface
22 investigations at contaminated sites, the effects to local shallow groundwater wells and
23 measurable influence on monitoring networks common at contaminated sites is unknown.
24 Physical and geochemical parameters associated with cone penetrometer testing were measured
25 from a transect of shallow groundwater monitoring wells upgradient and down-gradient of CPT
26 activity. The physical act of advancing and retracting a piezocone had a significant effect on
27 specific conductivity and water level but no effect on dissolved oxygen or pH. While cone
28 penetrometer effects were significant and detectable, the variability induced by CPT activity was
29 only a fraction of the natural variation caused by precipitation events. Therefore, we concluded
30 that CPT effects are less than those of natural event-driven variation in clayey and silty
31 unconsolidated residuum.

32

33 **Acknowledgement**

34 *This work was made possible by the effort and support of our Radiological Control Technicians*
35 *Mike Cooke and Alex Patton as well as our CPT rig operators Bobby Brandt and Tyrone*
36 *Sanders. We would like to thank Astrid Terry at Lawrence Berkeley National Laboratory and*
37 *thank Ryan Post and Firas Mishu at M&W drilling and Dennis Stauffer at Fugro for their*
38 *support and effort in securing contracts to complete this work. This material by ENIGMA-*
39 *Ecosystems and Networks Integrated with Genes and Molecular Assemblies a Science Focus*
40 *Area Program at Lawrence Berkeley National Laboratory is based upon work supported by the*
41 *U.S. Department of Energy, Office of Science, Office of Biological & Environmental Research*
42 *under contract number DE-AC02-05CH11231. Oak Ridge National Laboratory is managed by*
43 *UTBattelle, LLC, for the U.S. Department of Energy under contract DE-AC05-00OR22725.*

44

45 1. Introduction

46 Soil core recovery and penetration testing methods are essential in obtaining soil compaction,
47 stratigraphy, depth, porosity, and hydraulic conductivity for a variety of geotechnical and
48 engineering applications. While soil core recovery requires subsequent processing and
49 compaction corrections, penetration testing provides instant continuous data in-situ with a lower
50 relative cost, lower risk of cross contamination, and high accuracy. The reproducibility, speed,
51 and reliability of penetrometer testing in saturated material makes it a widely used and highly
52 standardized method for subsurface investigations^{1, 2}.

53 Cone Penetrometer Testing (CPT) is completed by advancing a cone-tipped pressure sensor
54 downward through unconsolidated material at a constant rate^{1, 2}. The CPT sensors are designed
55 to account for the eccentricity of push resistance such that the cone only measures the resistivity
56 imposed by the axial force of the soil layer which the cone is advancing through. Meaning that
57 the cones are optimized for variably compacted sediments particularly the fine grained residuum
58 which overlies the valley bedrock of the valley ridge formations common in the eastern
59 conterminous United States³. CPT probes can further incorporate additional sensors for
60 subsurface measurements including the monitoring of contaminants like hydrocarbons, volatile
61 organics, toxic metals, explosives/energetics, and radioactive wastes^{4, 5}. The CPT piezocone of
62 Figure 1 provides measures of soil friction f_s , resistance q_c , and pore pressure u_2 which are used
63 to interpret soil traits. Specifically soil type, which can be determined based on a relationship
64 between friction ratio, $R_f [R_f = (f_s/q_c) \times 100]$ and cone resistance, q_c ^{6, 7} with modern piezocones
65 providing corrected cone resistance q_t to account for pore water pressure in relation to net contact
66 area $a_n [q_t = q_c + u_2 (1 - a_n)]$ ⁸.

67 While the effectiveness of CPT is well documented, little is known of the immediate and
68 residual impacts of CPT activity on local hydrogeology and groundwater monitoring wells. The
69 effects of CPT were monitored during a CPT study completed at the contaminated Oak Ridge
70 Integrated Field Research Challenge Site within the Y-12 National Security Complex in Oak
71 Ridge, Tennessee, USA. A 2,600 square meter study site immediately down-gradient of the
72 former clay-lined S3 transuranic and nitric acid waste ponds was selected for study⁹. The site and
73 former S3 ponds are located in Bear Creek Valley, a valley and ridge province in Eastern
74 Tennessee, USA consisting primarily of clay and silt residuum deposited from the erosion of

75 local ridges (Figure S1). The unconsolidated sediments of Bear Creek valley overlie the
76 Maynardville Limestone which dips 45° to the southeast with a geologic strike of N55E⁹⁻¹¹. The
77 modern topography of the unconsolidated material is largely influenced by historical activities
78 which included grading, stream relocation, and the burial of debris recovered up to 4.1 meters
79 below ground surface^{9, 12}.

80 **2. Methods**

81 **2.1. Cone Penetrometer Testing**

82 Over 16 days in October of 2020, a 131-push cone penetrometer grid was completed across a
83 2,600 square meter site (Figure 2) with pushes advancing up to 11m below ground surface. A
84 255 square meter study site with pre-existing groundwater wells was the focus of studies
85 regarding CPT impacts on groundwater. Pushes North West of the 255 square meter subsite
86 region shown in Figure 3, were completed from October 13 through 18, 2020. The South Eastern
87 CPT boreholes including those in the study subsite (Table 2) were completed on October 18
88 through October 27, 2020. To collect subsurface data, a 25-ton CPT rig was driven to the bore
89 location and leveled. Then a 35.7 mm diameter piezocone was advanced through the subsurface
90 at a rate of 2 cm/sec with the use of a truck-mounted hydraulic ram. The piezocone advanced
91 below ground surface to collect soil behavior data in feet which were converted to meters by
92 dividing the depths by 3.281. The piezocone was advanced at a constant rate until the axial force
93 of the underlying material resulted in refusal after which the piezocone was retracted and the
94 resulting bore hole was left open until all bores had been completed for the day. After the
95 completion of daily CPT activities, the boreholes were sealed by gravity-feeding a saturated
96 sodium bentonite slurry until the bentonite was level with the ground surface.

97 **2.2. Water levels**

98 Three continuous-monitoring LevelTROLL® 400 depth to water units (In-situ, Fort Collins,
99 CO) were deployed in FW103, FW024, and FW112 at a depth of 12.2 -to- 15.2 m below ground
100 surface. Water level measurements were collected from the deployed units in ten minute
101 intervals for three months before the CPT, during the 16-days of CPT, and one-week post-CPT.

102 **2.3. Hydraulic Conductivity**

103 A subset of 5 groundwater wells screened from 6.1 -to- 15.2 m below ground surface and
104 identified in Table 2 were selected for hydraulic conductivity measurements (Figure 3). Two
105 methods of aquifer recharge were used to determine the groundwater flow rate using the
106 Hvorslev slug test method for unconfined aquifers¹³⁻¹⁵.

107

108
$$k = \frac{r^2 \ln(L/R)}{2Lt_{0.37}}$$

109

110 k = hydraulic conductivity
111 r = standpipe radius
112 L = screen length
113 R = sandpack radius
114 $t_{0.37}$ = time of 37% well recovery

115 Equation 1. Hvorslev equation for hydraulic conductivity in unconfined aquifers ¹³⁻¹⁵
116

117 One month-prior to the CPT, 5L of groundwater water was pumped from FW134-2, FW128,
118 and FW127 to clean the well screens and ensure no blockages were present. One-month post-
119 CPT, hydraulic conductivity slug tests were completed in FW127 and FW128 using a 1L
120 polypropylene slug to remove groundwater and measure recharge rate using an electric
121 conductivity water level tape with hydraulic conductivity calculated using the Hvorslev method
122 (equation 1). This method was also repeated for FW134-2 and FW115-3 using a 0.5L slug.
123 Steady-state drawdown was additionally achieved by pumping at a rate of <0.65 mL/sec in
124 FW115-3 on October 27th following the local CPT activity on October 24th and 25th. To measure
125 recovery, the pump was de-activated, and an electric water level tape was used to measure the
126 rate of recharge with hydraulic conductivity calculated using the Hvorslev method (equation 1).
127 In FW127, a colloidal borescope (Geotech, Denver, CO) was deployed to measure vector and
128 velocity of the 12.1 -to- 14.9 m screen interval. Prior to deployment a manual systems check was
129 performed including calibration of changing particle vector and velocity and optical calibration
130 tests. Particle tracking was measured using AquaVision software (Geotech, Denver, CO) and the
131 tracking parameters were adjusted to fit the clarity and conditions of the groundwater with
132 capture set to 100 milliseconds, the particle sensitivity filter set to 2000, a minimum particle size
133 set to 3 μm , maximum velocity capped at 5000 $\mu\text{m}/\text{sec}$, and a minimum threshold of two particle
134 matches for tracking. Flow was measured in a fracture 12.16 m below ground surface where
135 particle movement was observed over a 15-minute period.

136 **2.4. Continuous Geochemistry Monitoring below CPT pushes**

137 Continuous geochemistry was measured using an AquaTROLL® 600 multiparameter
138 sonde measuring groundwater in well FW 106, screened from 12.2 -to- 14.9 m below ground
139 surface. The AquaTROLL® 600 collected temperature ($^{\circ}\text{C}$), specific conductivity ($\mu\text{S}/\text{cm}$),
140 dissolved oxygen (mg/L), salinity (ppm), pH, and total suspended solids (ppt) every ten minutes.

141 All probes were calibrated prior to deployment on October 17th. Binomial-classified CPT activity
142 data were analyzed using an ANOVA test of variance with continuous geochemistry data from
143 FW106 and continuous water levels data from FW112.

144 **2.4.1. Geochemistry Monitoring at Depth of CPT**

145 On October 24th, geochemistry was measured from FW115-3 screened from 8.53 -to-
146 9.66 m below ground surface. Measurements were collected on an AquaTROLL® 9600 (In-situ,
147 Fort Collins, Co) treaded onto a flow cell. The unit was calibrated 4 hours before use and
148 measured temperature (°C), specific conductivity (μS/cm), dissolved oxygen (mg/L), and pH of
149 groundwater pumped peristaltically at a rate of 0.67 mL/sec. Three-times the volume of the
150 screen pack was pumped to establish a geochemistry baseline prior to the start of local CPT
151 activity, and a non-CPT measurement of the well was completed using the same method and re-
152 calibrated unit on October 27th.

153 3. Results and Discussion

154 3.1. Geochemistry effects of CPT

155 3.1.1. Geochemistry at Depth of CPT pushes

156 Prior to piezocone advancement and retraction, peristaltic pumping at an average rate of 0.67
157 mL/sec in FW115-3 established a geochemistry baselines for pH, dissolved oxygen, specific
158 conductivity, and temperature in groundwater. Stable parameter averages and standard deviations
159 before CPT activity showed a pH of 3.82 ± 0.01 , dissolved oxygen concentration of 0.12 ± 0.01
160 mg/L, a temperature of 22.11 ± 0.08 °C and specific conductivity of 3680 ± 15 $\mu\text{s}/\text{cm}$. Figure 4
161 shows the geochemistry data collected from FW115-3 during the CPT activity (excluding
162 temperature) with the mean during the October 24th CPT activity in teal, and the background
163 non-CPT mean from October 27th in gray. The means of pH and Oxygen during CPT activity
164 were equal to means from non-CPT measurements on October 27th. Specific conductivity
165 however was higher during CPT activity and peaked at 3799 $\mu\text{s}/\text{cm}$ during the development of
166 CPT47, the closest CPT borehole. The specific conductivity decrease was exponential (Figure 5)
167 and fit by the following second-order polynomial regression, $y = 1\text{E-}05x^2 - 0.0906x + 3691.4$
168 with an R-squared value of 0.98 where $x =$ volume pumped (mL) at a rate of 0.67 mL/minute
169 post-CPT and $y =$ specific conductivity ($\mu\text{s}/\text{cm}$ at 25°C).

170 3.1.2. Geochemistry Below CPT pushes

171 Continuous monitoring in FW106 indicated that specific conductivity and water level were
172 significantly affected during CPT activity (Table 3). Figure 6 shows that despite some local and
173 minimal variation in the underlying well, specific conductivity had a daily downward trend
174 preceding the CPT and during the CPT with daily highs recorded each morning and daily lows
175 recorded each night until a rain event on October 28th and 29th. The daily variation during the
176 CPT activity on October 24th and 25th was measured at 17 $\mu\text{s}/\text{cm}$ and 34 $\mu\text{s}/\text{cm}$ respectively.
177 While daily ranges in specific conductivity following 5.2 cm of rain of October 28th and 2.5 cm
178 of rain of October 29th demonstrated that the influence of precipitation on daily variability was
179 up to five-times that of the CPT (Figure 7). Overall, no influence to dissolved oxygen, or pH was
180 measured during or following the CPT activity in FW106.

181 3.2. Borehole stability and the effects of Bentonite

182 As the CPT piezocone advances, it displaces subsurface material and is capable of collapsing
183 open space between sediment grains and smearing fine grained clays along the edge of the

184 advancing piezocone. This smearing and compaction effect of the fine grained saprolite clay
185 material was demonstrated by cores collected using the same hydraulic press in the
186 unconsolidated residuum (Figure 8). The smearing effect and pore deformation was visually
187 limited to the outer 2 mm of the cores. The unconsolidated residuum materials tended to
188 collapse, back-filling the borehole and leading to possible sediment mixing across zones¹⁶. An
189 unknown number of boreholes did collapse during or immediately following the retraction of the
190 piezocone directly influencing the final depth of the sodium bentonite slurry. Sodium Bentonite
191 ($1_2H_2Na_2O_{13}Si_4$) has a pH of 8.5-10 and a high cation exchange capacity in groundwater
192 measurable by increases in pH and diversion from an existing trend in specific conductivity^{17, 18}.
193 However, the mean pH remained unaltered during the application of the sodium bentonite slurry.
194 The specific conductivity continued its downward trend in FW115-3 during the application of
195 the sodium bentonite slurry, and daily trends in FW106 had no detectable response.

196 **3.3. Local hydrologic effects**

197 Water levels are naturally attuned to precipitation events, as demonstrated by Figure 9. Seasonal
198 and event-driven water table fluctuations prior to the CPT result in regularly oscillating water
199 levels. However, unique variation events in FW112 resulted in deviations from the daily trend
200 during the CPT activity on October 18th, 24th, and 25th with water levels in flow-adjacent FW103
201 and FW024 not showing any fluctuations associated with local CPT activities. FW112 is local to
202 the CPT activity and roughly upgradient of the CPT activity based on groundwater vector
203 measured in FW127 and FW106. Figure 10 shows however, that the localized and short-term
204 fluctuations in FW112 water levels occurred during CPT activities in the overlying residuum on
205 October 24th. During piezocone advancement, the process displaced sediment and groundwater
206 increasing the local water level in FW112, and generated a void spaces estimated at 0.0112 m³,
207 0.0107 m³, and 0.0111 m³ for CPT49, CPT 47, and CPT 43 respectively. As the piezocone was
208 retracted, the void was filled by water from a recharging unit causing an observed decrease in
209 local water level. The water table elevation of FW112 in Figure 10 ranged from 304.40 -to-
210 304.47 m above mean sea level with a maximum water table fluctuation of 0.07 m during CPT
211 activities and water elevations stabilizing immediately following the CPT activity. On October
212 30th, following the rain event of October 28th and 29th, the total daily water level range in FW112
213 was 0.085 m indicating that the CPT water level variation is less than that of a precipitation
214 event. An ANOVA test of variance (Table 3) determined that water level in FW112 was

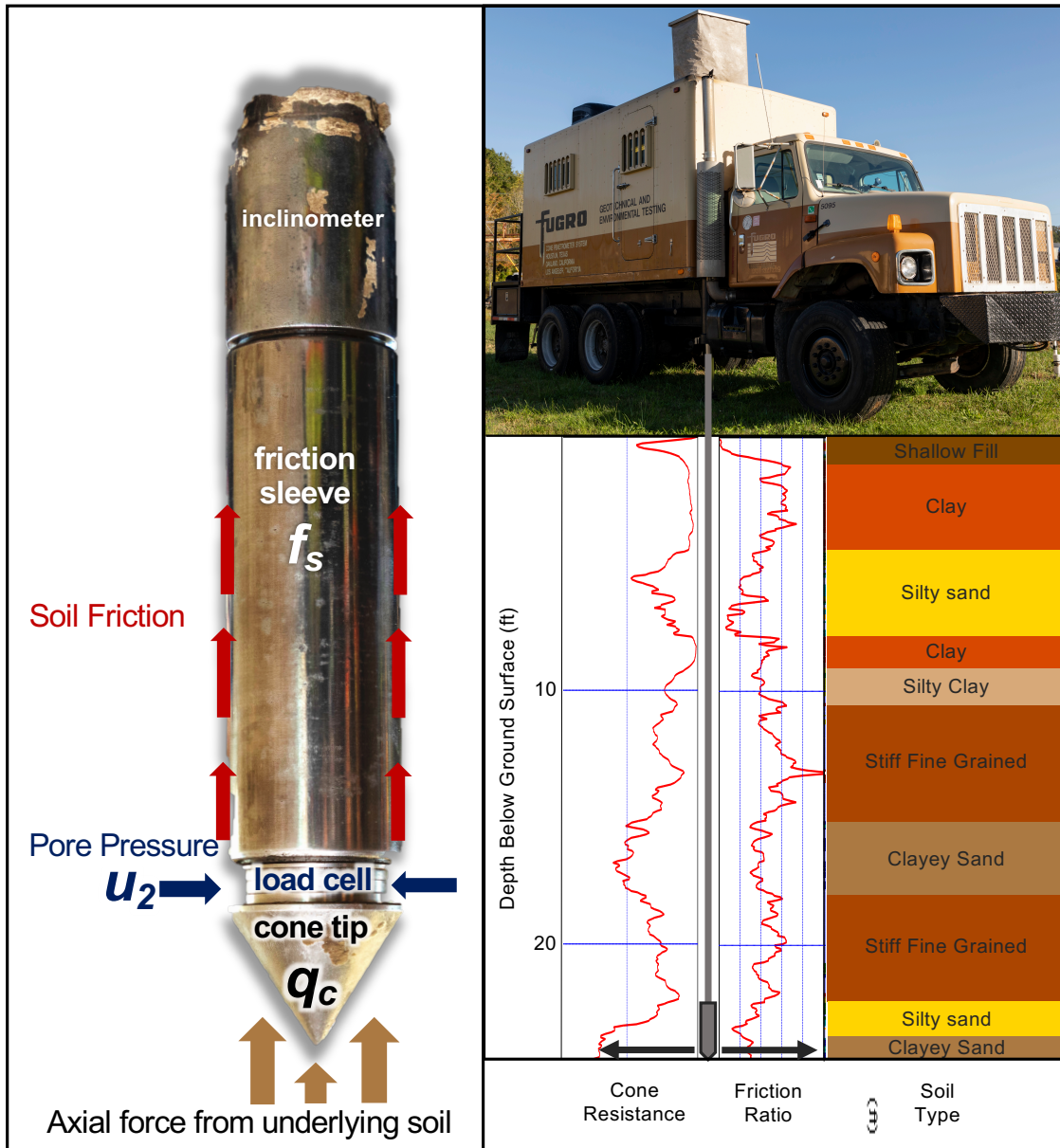
215 significantly influenced by physical advancement and retraction of a CPT piezocone. This highly
216 fractured material was very responsive to the CPT activity and recovered quickly, but rates of
217 recovery and radius of influence will vary based on local storativity, transmissivity, and
218 hydraulic conductivity. Across the saturated subsurface, hydraulic conductivity and permeability
219 at the site have been well-defined over several decades and have been determined to be between
220 10^{-6} -to- 10^{-7} m/sec in the shallow material 1-12 m below ground surface with underlying
221 fractures providing flow up to 10^{-2} m/sec⁹. Three days post-CPT, hydraulic conductivity in
222 FW115-3 was determined to be 1.22×10^{-7} m/sec and 6.60×10^{-7} m/sec one month later. One-
223 month following the CPT, hydraulic conductivities of the shallow unconsolidated residuum were
224 remeasured and ranges were all within the expected for the material (Table 2) indicating that any
225 impacts of subsurface cavities, or compaction were not present or negligible on overall hydraulic
226 conductivity. While physical disruptions to subsurface structures and grain-to-grain relationships
227 can alter flow paths, tortuosity, and Reynolds numbers for the material, the CPT did not have a
228 measurable impact on local hydraulic conductivity¹⁶.

229 **3.4. Overall Assessment of CPT Effects**

230 The process of advancing and retracting the CPT probe significantly affected water level,
231 specific conductivity, salinity, and oxidative reductive potential in underlying wells. At depth of
232 the CPT, specific conductivity increased above background as CPT activity neared the
233 monitoring well reaching a local maxima of 3799 $\mu\text{s/cm}$. However, a rain event at the site
234 resulted in a peak specific conductivity of 3979 $\mu\text{s/cm}$ in FW106. The CPT daily variation in
235 specific conductivity in FW106 was a fifth of the daily variation measured following a rainfall
236 event at the site. The rainfall also resulted in a maximum daily water level variation of 0.08 m
237 while the CPT resulted in only a daily variation of 0.07 m. Means for pH and dissolved oxygen
238 did not vary from background and sealing of the boreholes with the sodium bentonite slurry had
239 no measurable effect on groundwater geochemistry. This suggests that the effects of the CPT
240 advancement and retraction have a limited impact on the local hydrogeology, but that the effects
241 and influence on each measured geochemical and physical parameter was less than that of a
242 rainfall event.

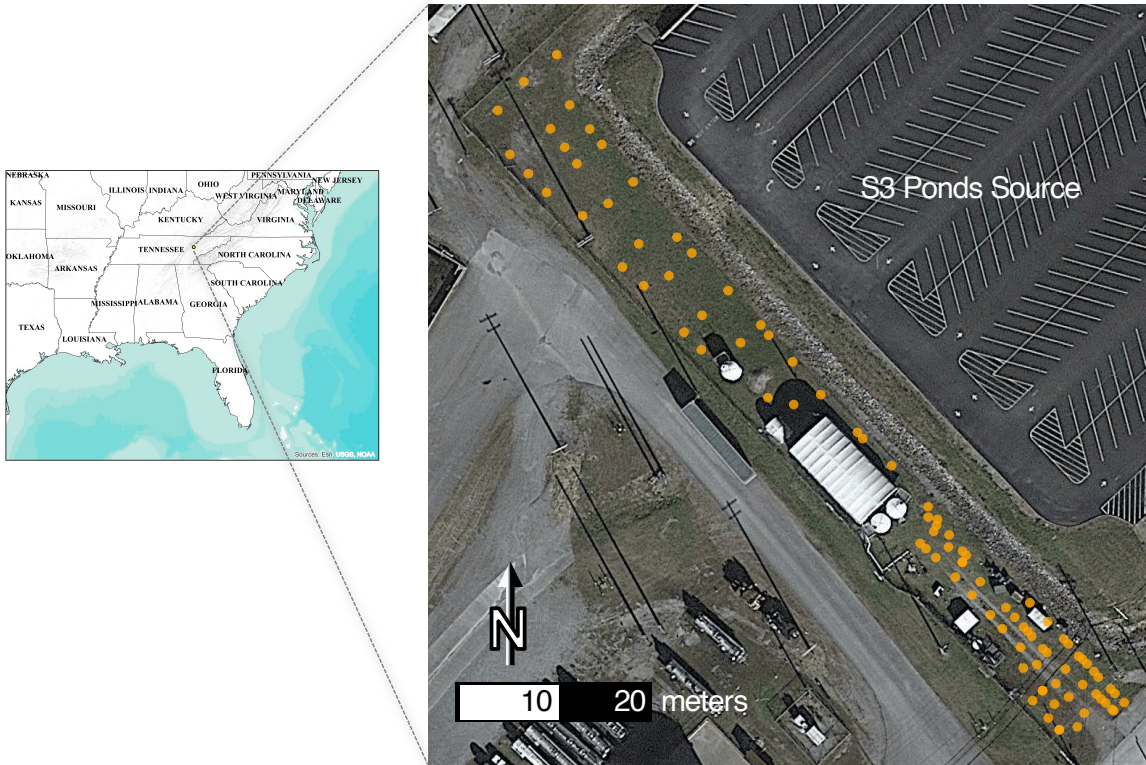
References

- 244 1. International, A., D6067/D6067M-17 Standard Practice for Using the Electronic
245 Piezocone Penetrometer Tests for Environmental Site Characterization and Estimation of
246 Hydraulic Conductivity. ASTM International: West Conshohocken, PA, 2017.
- 247 2. International, A., D5778-20 Standard Test Method for Electronic Friction Cone and
248 Piezocone Penetration Testing of Soils. ASTM International: West Conshohocken, PA,
249 2020.
- 250 3. Hoos, A. B., *Reconnaissance of surficial geology, regolith thickness, and configuration*
251 *of the bedrock surface in Bear Creek and Union Valleys, near Oak Ridge, Tennessee*. US
252 Department of the Interior, Geological Survey: 1986; Vol. 86.
- 253 4. Doskey, P. V.; Cespedes, E. R., Cone-penetrometer-deployed Samplers and Chemical
254 Sensors. *Encyclopedia of Analytical Chemistry* **2006**.
- 255 5. Malone, P. G.; Comes, G. D.; Chrestman, A. M.; Cooper, S. S.; Franklin, A. G., Cone
256 Penetrometer Surveys of Soil Contamination. *Environmental Geotechnology* **1992**, 251-
257 257.
- 258 6. Robertson, P., Soil classification using the cone penetration test. *Canadian Geotechnical*
259 *Journal - CAN GEOTECH J* **1990**, 27, 151-158.
- 260 7. Schmertmann, J. H., Guidelines for cone penetration test : performance and design. **1978**.
- 261 8. Robertson, P. K. In *Soil behaviour type from the CPT: an update*, 2nd International
262 symposium on cone penetration testing, 2010; pp 575-583.
- 263 9. Watson, D.; Kostka, J.; Fields, M.; Jardine, P., *The Oak Ridge Field Research Center*
264 *conceptual model*. 2004.
- 265 10. Hatcher, R. D., Jr.; Lemiszki, P. J.; Foreman, J. L.; Dreier, R. B.; Ketelle, R. H.; Lee,
266 R. R.; Lee, S. Y.; Lietzke, D. A.; McMaster, W. M. *Status report on the geology of the*
267 *Oak Ridge Reservation*; United States, 1992; p 271.
- 268 11. Oak Ridge Y-12 Plant, T. N. *Calendar year 1994 groundwater quality report for the*
269 *Bear Creek hydrogeologic regime, Y-12 Plant, Oak Ridge, Tennessee 1994 Groundwater*
270 *quality data interpretations and proposed program modifications*; United States, 1995; p
271 300.
- 272 12. Sutton Jr, G.; Field, S. *Distribution of anthropogenic fill material within the Y-12 Plant*
273 *Area, Oak Ridge, Tennessee*; Oak Ridge Y-12 Plant, TN (United States): 1995.
- 274 13. Bouwer, H.; Rice, R. C., A slug test for determining hydraulic conductivity of unconfined
275 aquifers with completely or partially penetrating wells. *Water Resources Research* **1976**,
276 12 (3), 423-428.
- 277 14. Hvorslev, M. J., *Time lag and soil permeability in ground-water observations*.
278 Waterways Experiment Station, Corps of Engineers, US Army: 1951.
- 279 15. Weight, W., *Hydrogeology field manual*. McGraw-Hill Education: 2008.
- 280 16. Aller, L., *Handbook of suggested practices for the design and installation of ground-*
281 *water monitoring wells*. Environmental Monitoring Systems Laboratory, Office of
282 Research and ...: 1991; Vol. 1.
- 283 17. Barcelona, M. J.; Gibb, J. P.; Miller, R. A., *A guide to the selection of materials for*
284 *monitoring well construction and ground-water sampling*. Illinois State Water Survey:
285 1983; Vol. 327.
- 286 18. Enforcement, U. S. O. o. W. P., *RCRA Ground-water Monitoring Technical Enforcement*
287 *Guidance Document (TEGD)*. U.S. Environmental Protection Agency, Office of Waste
288 Programs Enforcement, Office of Solid Waste and Emergency Response: 1986.



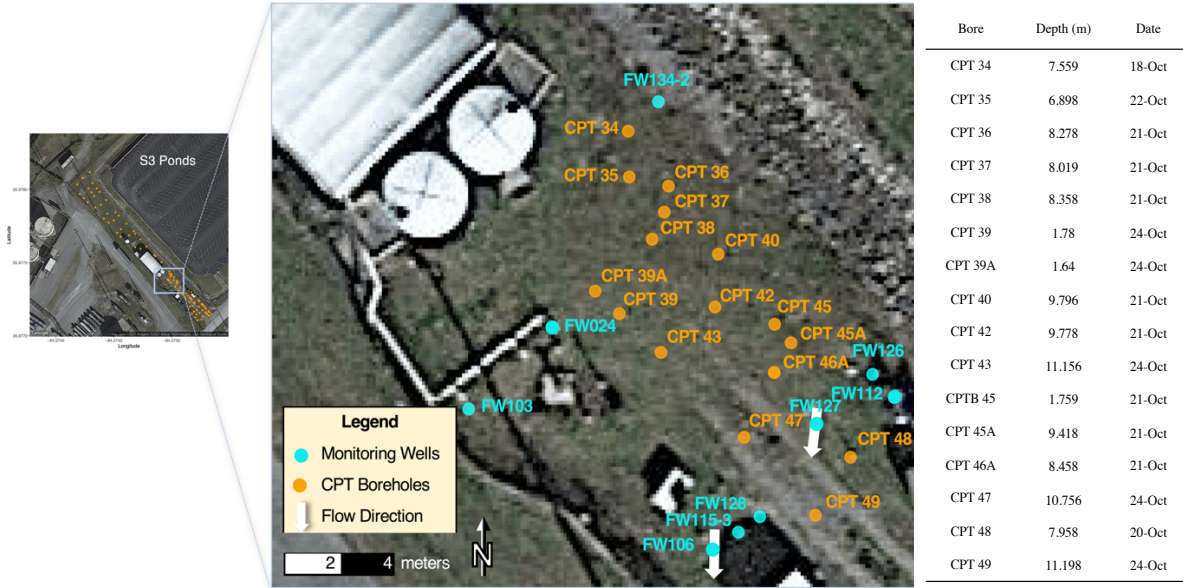
290

291 **Figure 1.** Piezocone sensors (left) measure the axial force on the cone, the upward bore wall
 292 friction, and the inward pore pressure to determine soil behavior which is interpreted during
 293 subsurface piezocone advancement (right).



294

295 **Figure 2.** The cone penetrometer study was conducted in the 2,600 square meter Area 3 site
 296 at the Y-12 complex in Oak Ridge, TN, USA. Boreholes shown in orange form parallel
 297 transects downgradient of the former S3 waste ponds contaminant source.



298

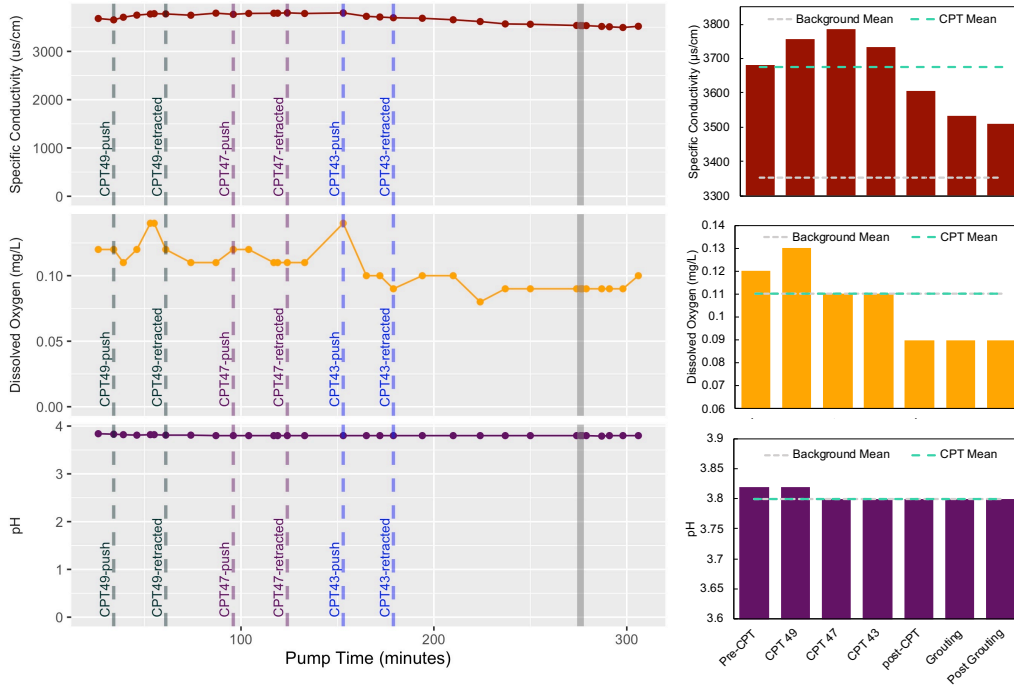
299

300

301

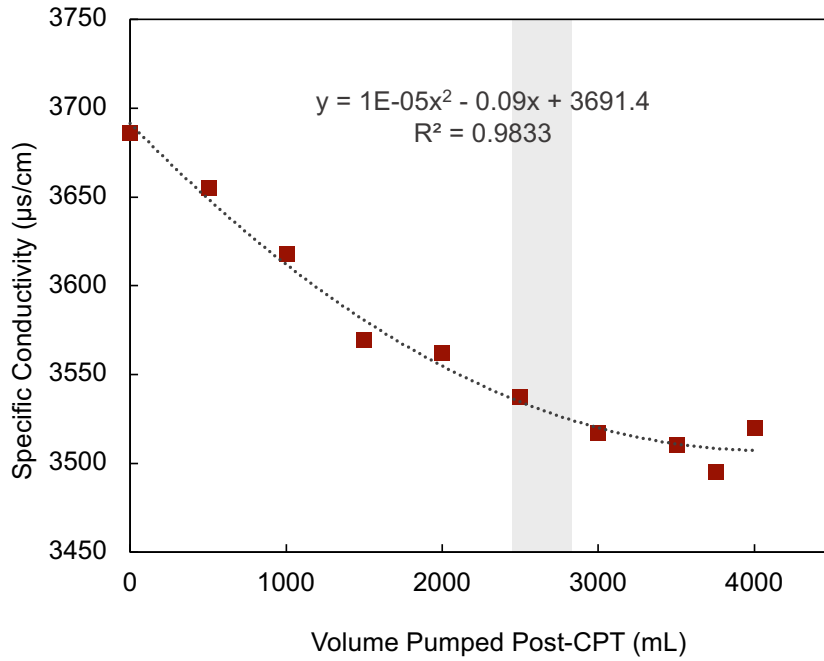
302

Figure 3. Map of cone penetrometer bore holes and monitoring wells used to investigate the localized effects of the CPT in Area 3. Flow direction arrows were drawn from vectors collected using colloidal borescope and indicate a southerly groundwater flow in the residuum.



303
 304
 305
 306
 307

Figure 4. Geochemistry measured in FW115-3 throughout local cone penetrometer activities are shown on the right with boreholes grouted around 270 minutes (charcoal). Mean values for CPT activity are plotted in the bar charts on the right with mean during CPT activity in teal and mean non-CPT geochemistry background in ash.

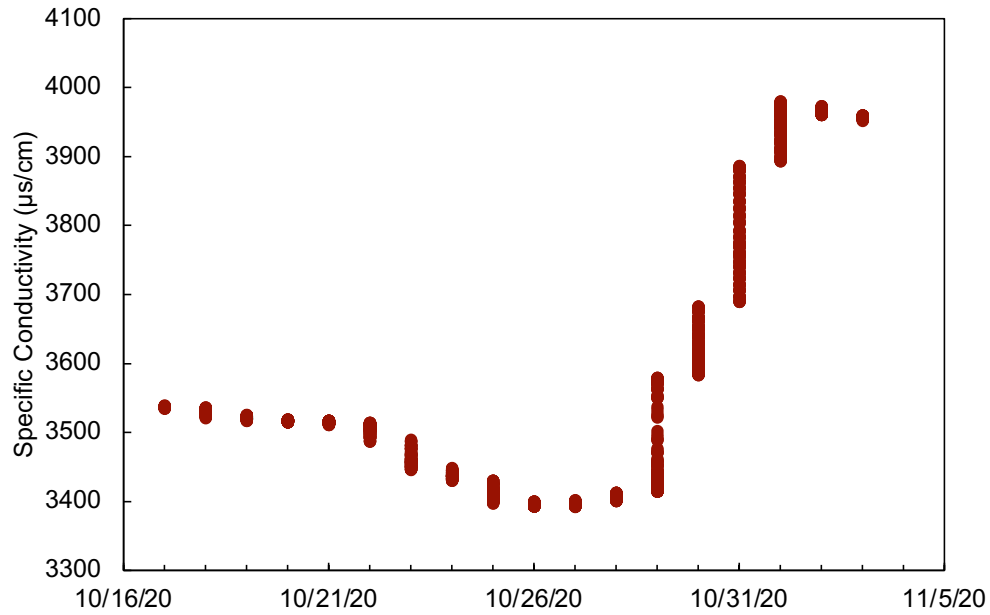


308

309

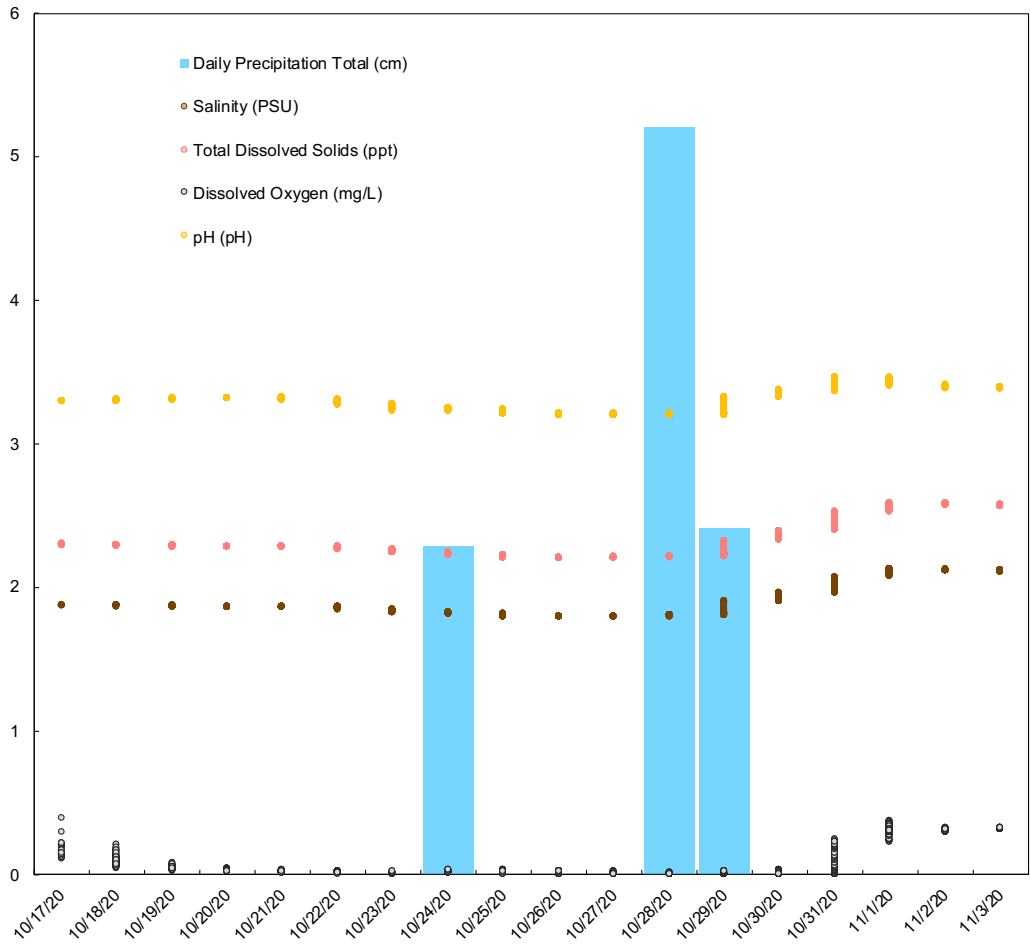
310

Figure 5. Specific conductivity decrease following the localized cone penetrometer activity including during the addition of a bentonite slurry (charcoal) in CPT 43, 47, and 49.



311

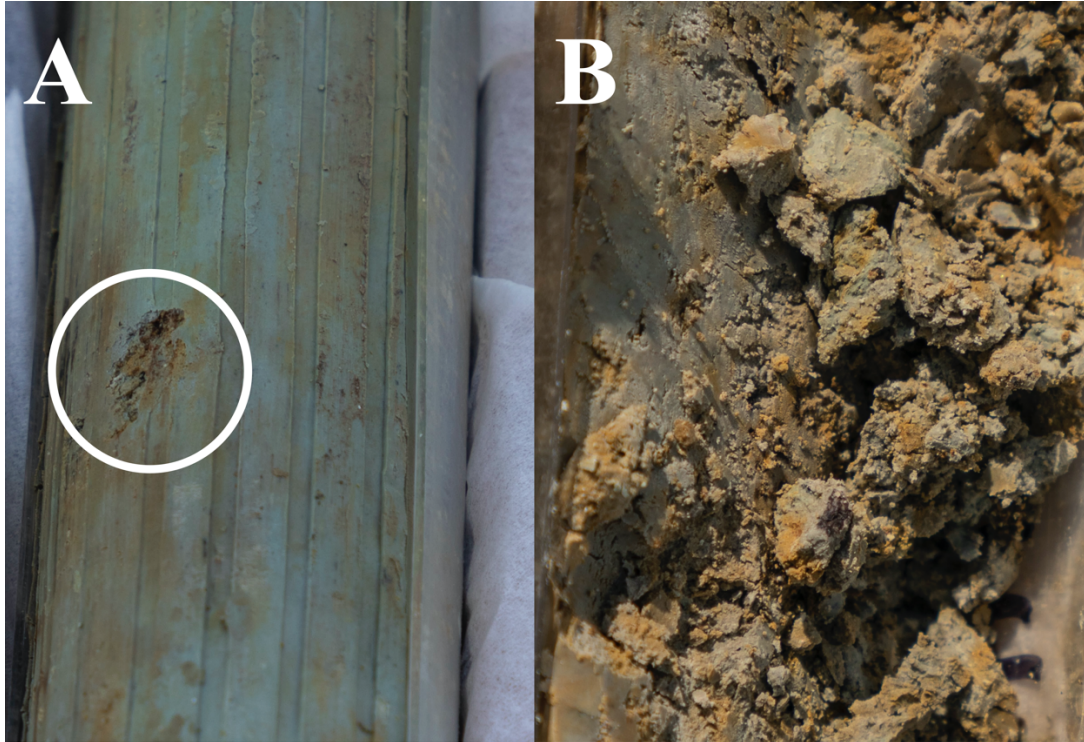
312 **Figure 6.** Groundwater specific conductivity continuous monitoring of underlying
 313 groundwater well FW106. Measurements collected every 10 minutes are plotted as daily
 314 ranges with dates recorded in month/day/year. CPT activities localized to FW106 took place
 315 on 10/18/20, 10/20/20 – 10/22/20, 10/24/20 and 10/25/20. On 10/28/20 the site received 5.2
 316 centimeters of rain and an additional 2.5 centimeters on 10/29/20 after which the specific
 317 conductivity increased daily until stabilizing on 11/02/20.



318

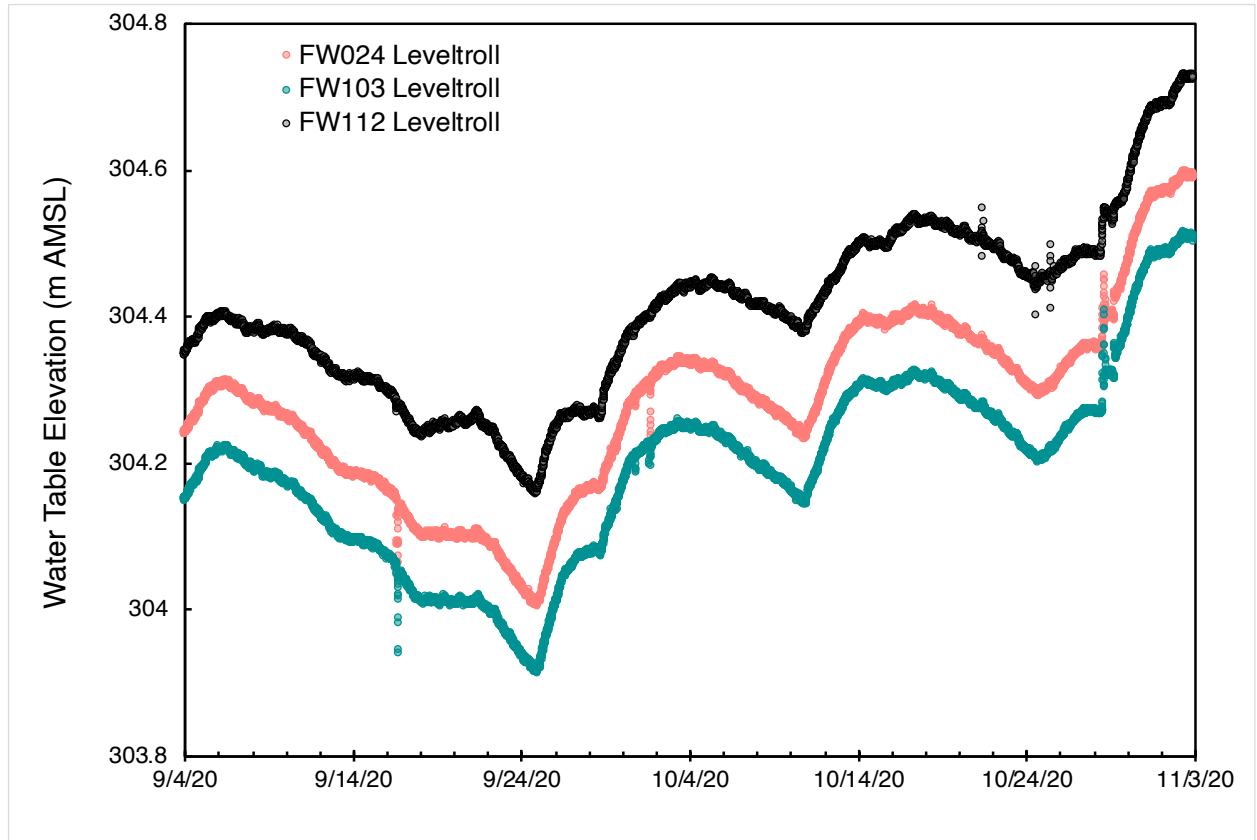
319
 320
 321
 322
 323
 324

Figure 7. Continuous monitoring data collected every 10 minutes are plotted as daily ranges with dates recorded in month/day/year from FW106 for all parameters except specific conductivity. CPT activities upgradient of FW106 took place on 10/18/20, 10/20/20 – 10/22/20, 10/24/20 and 10/25/20. On 10/28/20 the site received 5.2 centimeters of rain and an additional 2.5 centimeters on 10/29/20 resulting in a higher daily variability until stability was achieved around 11/02/20.



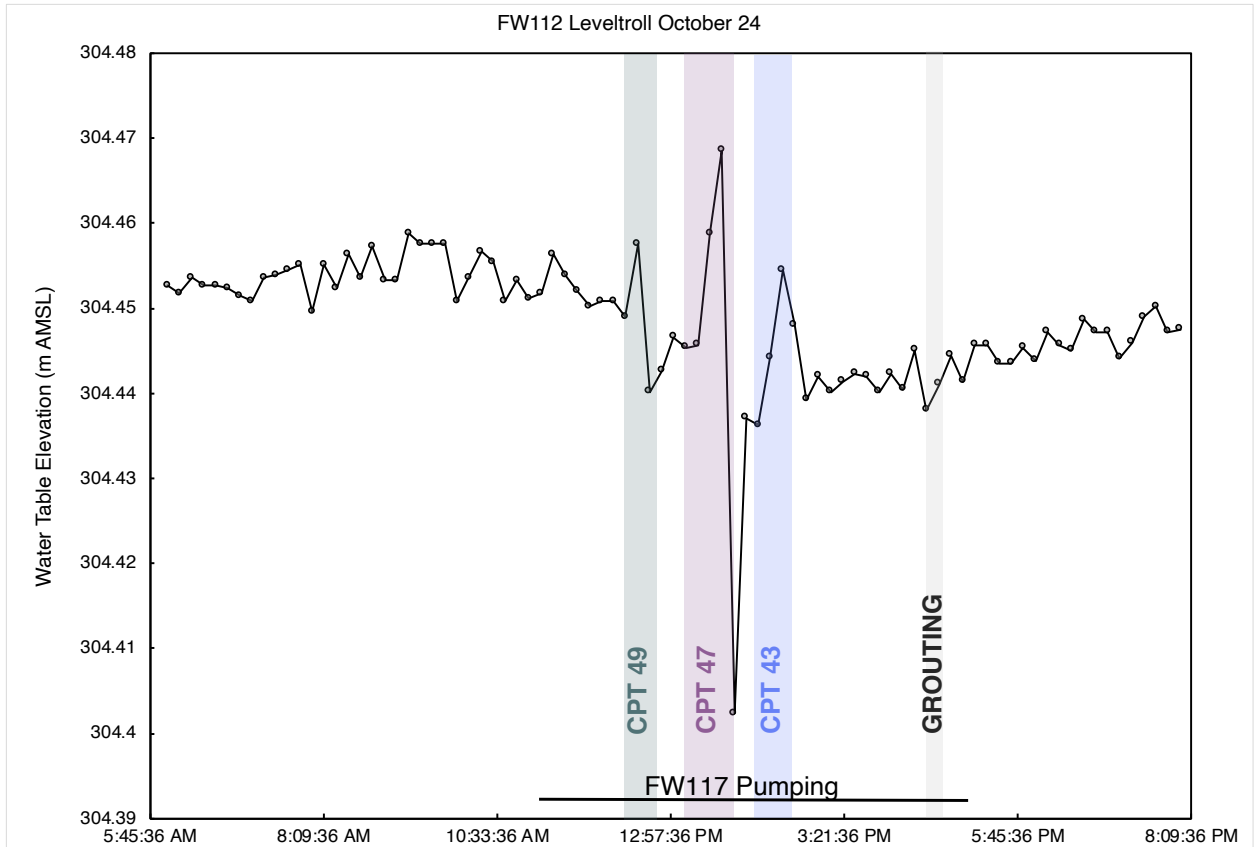
325
326
327
328
329

Figure 8 Sediment collected from the unconsolidated residuum where (A) pore compaction was caused by the advancement of the probe against (B) the typical material structure of the clayey residuum. The white circle shows a window into the core ~2 mm deep demonstrating the limited extent of the pore compaction and smearing.



330
 331
 332
 333
 334
 335
 336
 337

Figure 9. Continuous water level data from FW024, FW103, and FW112 collected in 10 minute intervals and recorded as month/day/year demonstrates the oscillating pattern of water level change common under ambient conditions. Local CPT activities occurred on 10/18/20, 10/20/20 – 10/22/20, 10/24/20 and 10/25/20. Observable water level variation is exhibited in FW112 from local CPT activities on 10/21/20, 10/22/20, 10/24/20 and 10/25/20. On 10/28 the site received 5.2 centimeters of rain and an additional 2.5 centimeters on 10/29 resulting in the rising water levels after 10/28/20.



338
 339
 340
 341
 342

Figure 10. Continuous water level data from FW112 demonstrating the water level fluctuations of local CPT activities on 10/24/20. Each bar represents the CPT push and retraction with downward advancement occurring in the first half of each bar and retraction occurring in the later half.

343 **Tables**

344 **Table 1.** CPT subsite borehole depths and date of completion

Bore	Depth (m)	Date
CPT 34	7.559	18-Oct
CPT 35	6.898	22-Oct
CPT 36	8.278	21-Oct
CPT 37	8.019	21-Oct
CPT 38	8.358	21-Oct
CPT 39	1.78	24-Oct
CPT 39A	1.64	24-Oct
CPT 40	9.796	21-Oct
CPT 42	9.778	21-Oct
CPT 43	11.156	24-Oct
CPTB 45	1.759	21-Oct
CPT 45A	9.418	21-Oct
CPT 46A	8.458	21-Oct
CPT 47	10.756	24-Oct
CPT 48	7.958	20-Oct
CPT 49	11.198	24-Oct

345

346

Table 2. Local hydraulic conductivity

well	screen interval (m)	local CPT depth (m)	well proximity to CPT	method	<i>k</i> (m/sec)
FW134-2	6.1 – 7.6	7.6	upgradient	0.5 L Slug	2.59×10^{-6}
FW115-3	8.5 – 9.7	10.8	down-gradient	0.5 L Slug	6.60×10^{-7}
FW115-3	8.5 – 9.7	10.8	down-gradient	Pump	1.22×10^{-7}
FW128	12.4 – 15.1	10.8	down-gradient	1 L Slug	1.01×10^{-5}
FW103	11.27 – 13.7	1.8	down-gradient	1 L Slug	2.65×10^{-5}
FW127	12.16 – 15.1	9.4	down-gradient	Borescope	1.77×10^{-4}

347

348

349 **Table 3.** ANOVA test of variance results

	Sum of Squares	F-value	p-value	Significance
FW112 Water Level	0.743	10.36	0.002	**
Temperature	0.004	0.052	0.821	
Specific Conductivity	0.427	5.954	0.016	*
Salinity	0.355	4.957	0.028	*
Total Suspended Solids	0.026	0.357	0.551	
Resistivity	0.008	0.108	0.743	
Barometric Pressure	0.176	2.448	0.120	
pH	0.166	2.316	0.130	
Oxidative Reductive Potential	0.671	9.364	0.003	**

350 *p<0.05 **p<0.01